Effect of thickness on structural, optical and magnetic properties of Co doped ZnO thin film by pulsed laser deposition

A. KAMALIANFAR[a,b], S. A. HALIM[a,c*], KASRA.BEHZAD[a], MAHMOUD GOODARZ NASERI[a], M. NAVASERY[a], FASIH UD DIN[a], J. A. M. ZAHEDI[d] , K.P.LIM[a], S.K.CHEN[a], H.A.A.SIDEK[a]
[a]*Department of Physics, Faculty of Science, Universiti Putra Malaysia, 43400 UPM, Serdang, Selangor , Malaysia.*
[b]*Department of Physics, Faculty of Science, University of Jahrom, Jahrom,* 66171-74137*, Iran.*
[c]*Institute for Mathematical Research, Universiti Putra Malaysia, 43400 UPM, Serdang, Selangor, Malaysia*
[d]*Department of Physics, Karaj Branch, Islamic Azad University, Karaj, Iran.*

$Zn_{0.97}Co_{0.03}O$ thin films were deposited on n-type silicon substrate (111) using pulsed laser deposition (PLD) technique with different thicknesses of $200 \pm 20nm$, $320 \pm 20nm$, and $480 \pm 20nm$. The $Zn_{0.97}Co_{0.03}O$ powders prepared by sol-combustion were formed as pellets. A neodymium-doped yttrium aluminum garnet (Nd:YAG) class 4 laser (λ = 266 nm, 5-8 pulse duration, 2 Hz duration rate) were used for the PLD of the nanostructures. The structure of the prepared thin films was investigated using different techniques such as X-ray diffraction (XRD) and field emission scanning electron microscope (FESEM). The optical properties of prepared thin films were investigated using UV-vis spectrometry. In addition, the magnetic properties of the samples were studied by vibrating sample magnetometer (VSM). The results showed that the properties of the thin films altered by thickness changes.

(Received August 24, 2012; accepted April 11, 2013)

Keywords: Co-doped ZnO, Thin Film, PLD, Dilute magnetic semiconductor

1. Introduction

Recently, the potential for some applications in spintronics has attracted wide research on dilute magnetic semiconductor (DMS). The main idea of DMS is to dope transition metal ions (e.g. Mn, Co or Fe) into a semiconductor host to prepare magnetic semiconductor at room temperature [1],[2],[3],[4]. It is supposed to have good control on the spin as well as electron charge for next generation spintronics devices. Some properties of ZnO such as wide band gap energy (~3. 37ev), transparency to visible light and chemical compatibility with other oxidizing materials provide a potential for the usage in magneto optical devices [5]. A variety of methods have been used to synthesize doped and undoped ZnO semiconductors including sol-gel [6], Spin-Coating Technique [7], pulsed laser deposition (PLD) [8], [9], [10] and vapor phase transport (VPD [11]. Among these methods, pulsed laser deposition method is a versatile technique and allows deposition different materials, e.g. high-temperature superconductors and oxides with high deposition rates.

Here, we study the effect of thickness on the structural, optical and magnetic properties of $Zn_{0.97}Co_{0.03}O$ thin films. PLD technique was chosen and three Co doped ZnO thin films were prepared.

2. Experimental

$Zn_{0.97}Co_{0.03}O$ powder was prepared by sol-combustion method [12]. The powder was pressed in a form of pellet and sintered at 600 ˚C for 1h to be used as a target. The silicon substrates were cleaned by HCl, NH3 and acetone before being placed onto the sample holder. A Nd:YAG laser system (λ=266 nm, 5-8 ns of duration pulse, 2 Hz of repetition rate and 0.5 J/cm^2 fluence of energy) was used to deposit three $Zn_{0.97}Co_{0.03}O$ thin films with different thicknesses. The background pressure of the vacuumed chamber was 10^{-5}mbar. The deposition was carried out in an oxygen atmosphere about 0.15 mbar instead of nitrogen due to the incorporation of nitrogen affecting the properties of the DMS material [13],[14]

The temperature of the substrates was fixed at 600 ˚C while the holder of the target was rotated slowly to obtain better thin films crystalline and homogeneity. A post-deposition annealing at 550 ºc was applied to decrease oxygen vacancies and the samples were cooled to room temperature at 8 ˚C/min rates. Using a high surface profilometer (Ambios, XP-200), the thickness of the films was estimated about $200 \pm 20nm. 320 \pm 20nm,\ 480 \pm 20nm$. The structural analysis of the samples was performed using X-ray diffraction (XRD, Pw 3040 MPD) with energy dispersive X-ray spectrometer (EDX). The morphology of the samples was observed by field emission scanning electron microscopy (FESEM, JSM

6700). To characterize the optical properties, Ultraviolet-visible spectroscopy (UV-vis, Perkin Elmer 360 Shimazu) was performed on the samples in the wavelength range 200-800nm at room temperature. Their Magnetic measurements were done using vibrating sample magnetometer (VSM, Lake Shore 4700) at room temperature.

3. Results and discussion

3.1 Structures and morphology of the Co doped ZnO films

Fig. 1 shows the XRD patterns of the Co doped ZnO thin films deposited on silicon substrates by PLD method at temperature 600°C. The main peaks of the ZnO wurtzite structure can be seen in all of the patterns. According to XRD patterns and Table 1, it can be found that longer deposition time causes more intensity of peaks due to the increase of the thickness of the film.

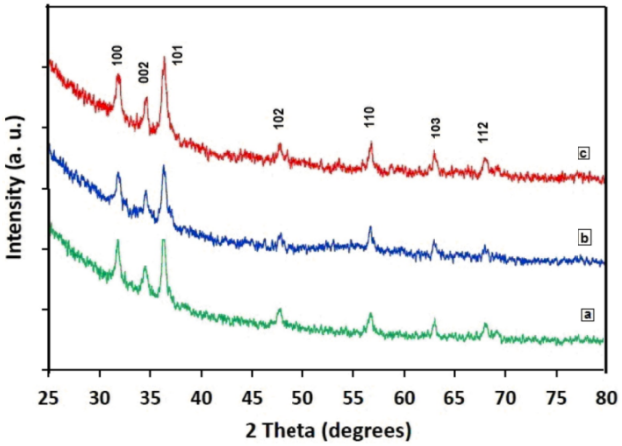

Fig. 1. XRD patterns of the prepared films with thicknesses of (a) 200 nm (b) 320 nm (c) 480 nm.

The corresponding peaks to cobalt oxide do not appear in the patterns because of its low concentration in the composite. A typical EDX obtained from the second sample is shown in Figure 2. As can be seen, Zn, O and Co elements were detected in all the thin films with different thicknesses. While the EDX pattern proves the presence of cobalt, the absence of Co or CoO peaks in the XRD pattern(Fig. 1), indicates that Co ion substitution with Zn^{2+} has not changed the wurtzite structure of ZnO with a low (3%) concentration of cobalt.

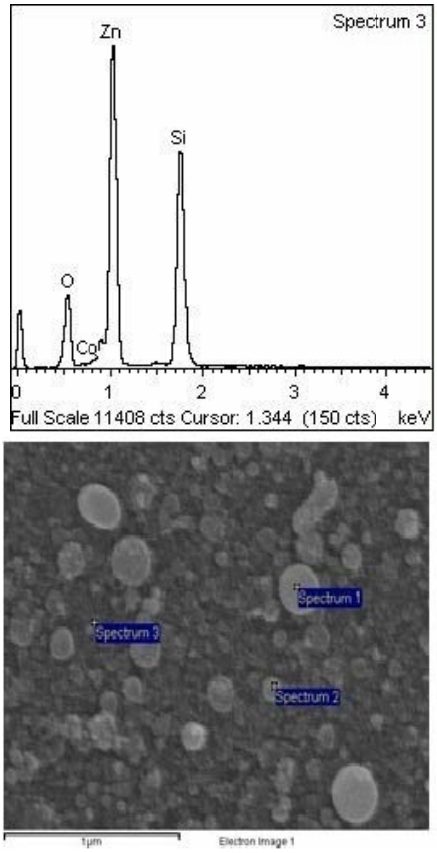

Fig.2. EDX of the thin film with thickness of 320 .

The (002) peak was chosen to estimate the crystallite size (D) and dislocation density (δ) from the FWHM (β) related to the films with different thickness. To calculate the crystallite size (D), we used Debye Scherrer's formula [15]:

$$D = \frac{0.94\lambda}{\beta\cos(\theta)} \quad (1)$$

where λ is the source wavelength, β is the diffraction line broadening at half the maximum intensity (FWHM) of the peak, and θ is the peak position. Using the grain size and the formula below [16], we obtained the dislocation density (δ) corresponding to the amount of the film defects,

$$\delta = \frac{1}{D^2} \quad (2)$$

The results are presented in Table 1. By increasing the thickness of the films, the diffraction peak of (002) clearly shifts a little toward the lower diffraction angles, and their FWHM declines due to change of the crystallite size. With a smaller value of δ (the lower defect) or larger value of D, the crystallization of the thin films is obviously enhanced. Thus, comparing the films with different thickness, the film with 480nm thickness has better crystallization.

Table 1. Comparison of position, height, FWHM, crystallite size and dislocation density of (002) diffraction peaks.

No.	Position angle (2θ)	Height (CTs)	FWHM (θ)	Crystallite size (nm)	Dislocation density (10^{-4} nm^{-2})
(a) $200 \pm 20nm$	35.51	20.93	0.5723	15.22	43.14
(b) $320 \pm 20nm$	34.50	21.98	0.4149	20.94	22.80
(c) $480 \pm 20nm$	34.42	22.04	0.3046	28.52	12.30

For magneto-optic applications, surface properties are significant factors that influence some optical and magnetic properties. Fig. 3 shows the morphology of the surface of thin films after annealing at 550˚C for 1 h under O2 gas flow. All the images were obtained by field emission scanning electron microscopy (FESEM). The size distribution diagram for the particles is shown below the FESEM images. As observed in the images, for the thin film with 200 ± 20nm thickness, the mean size of particles is 14.75±0.03 nm, whereas for 320 ± 20nm and 480 ± 20nm thicknesses, the mean size of particles are 19.01±0.03nm, 28.13±0.03 nm respectively. It can be stated that the particles have probably more freedom directions for growth when the thickness of film increases, so the size of particles will be larger.

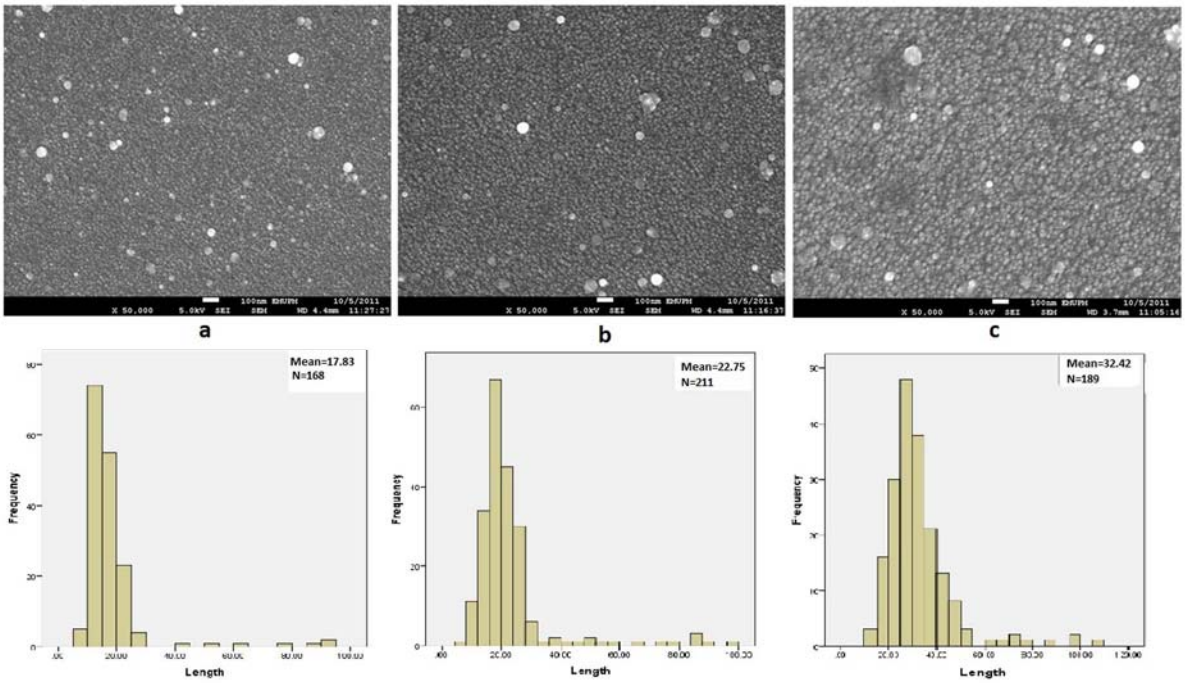

Fig.3. FESEM images their histogram particle size diagrams of the films with thicknesses of (a) $200 \pm 20nm$ *(b)* $320 \pm 20nm$ *(c)* $480 \pm 20nm$

3.2 Optical characteristics

The variation of thickness of Co doped ZnO layers and the growth temperatures have significant effect on the optical properties and crystalline structure. To investigate the film thickness effect on the energy band gap values, the $(\alpha h\nu)^2$ versus ($h\nu$) of absorption spectra in the range of 200 and 800 NM was plotted, where α is the absorption coefficient and hν is the photon energy. Figure 4 presents variation of the energy band gap for different film thicknesses. It indicates that by increasing the thickness of the films, the band gap energy values decrease from 3.27 to 3.32 eV. This variation of the band gap values can be related to decreasing the crystalline size of thin films because the crystalline size rises with increases of the film thickness (quantum size effect). This change can also be attributed to the improvement in the crystals, changes of structural defects, atomic distances and grain size in the films. The inset shows the absorption spectra of the samples.

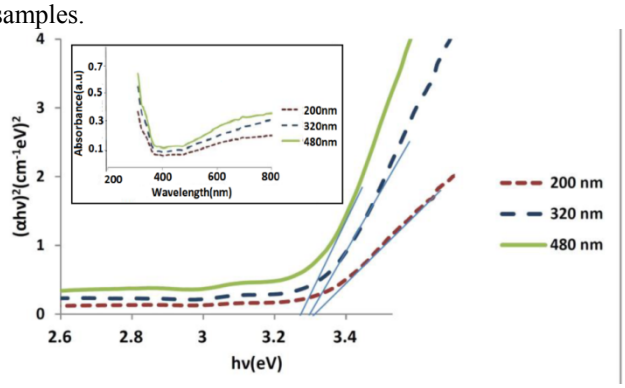

Fig.4. Variation of $(\alpha h\nu)^2$ *versus hν for* $Zn_{0.97}Co_{0.03}O$ *thin films with different thicknesses.*

3.3 Magnetic characteristics

Fig 5 shows the field-dependent magnetization (M–H) of the $Zn_{0.97}Co_{0.03}O$ samples with different thicknesses at room temperature. As a point of comparison, the magnetization of two other ZnO films with 6 and 9 percent of cobalt was shown as well. The diamagnetic ratio due to Si substrate was subtracted out of the obtained data. As can be seen, the $Zn_{0.97}Co_{0.03}O$ films exhibit weak ferromagnetic behavior. The curves of (d) and (e) shows the field-dependent magnetization of the $Zn_{0.94}Co_{0.06}O$ and $Zn_{0.91}Co_{0.09}O$ films with a similar thickness ($\sim 440 \pm 20nm$ and $550 \pm 20nm$) but with more concentration of Co. Hence, the films show a stronger ferromagnetic behavior. The question here is : what causes a room temperature ferromagnetism in a DMS material? Based on ZnO semiconductors with defects, the Ruderman–Kittel–Kasuya–Yosida (RKKY) model was employed by Story et al. [17] to explain the exchange coupling energy. Thus, the effective magnetic Hamiltonian is given by this equation:

$$H = \sum_{ij} J_F(r_{ij})\vec{S}_i \cdot \vec{S}_j + \sum_{ij} J_{AF}(r_{ij})\vec{S}_i \cdot \vec{S}_j + \sum_{ij} J_F'(r_{ij}) S_i \cdot S_j \quad (3)$$

In this equation, J_F is the parameter of ferromagnetic coupling between the magnetic ions, J_{AF} is the antiferromagnetic coupling parameter between them and J_F' is the ferromagnetic coupling parameter for the impurities and localized carriers. The spatial distance between randomly located substitutional magnetic pair in the lattice (r_{ij}) and the impurity spins (S_i, S_j) are other parameters considered.

Therefore, the room ferromagnetic behavior originates from three parts. One of them is direct interaction between magnetic ions (antiferromagnetic coupling) and two others are indirect couplings between the bound magnetic polaron mode and delocalized carriers or weak localized carriers. These two couplings provide ferromagnetic alignment inside the lattice. According to [18], for the samples with an absolute moment less than 5 μemu, the moment comes from extrinsic sources including substrate effect. Liu et al. [19] reported that the oxygen vacancies contribute to an indirect interaction with the bound magnetic polarons model and provide the ferromagnetic behavior of Co doped Zno. They also mentioned that the ferromagnetism is not due to metalic cobalt clusters.

Although, the Co ions of Co doped ZnO can cause the small amount of absolute moment, but the possibility of the mismatch coupling between Co spin orientation and donor electron states for the room temperature ferromagnetic cannot be ruled out. In addition, the Co doped ZnO has this ability to present strong room temperature ferromagnetism [20].

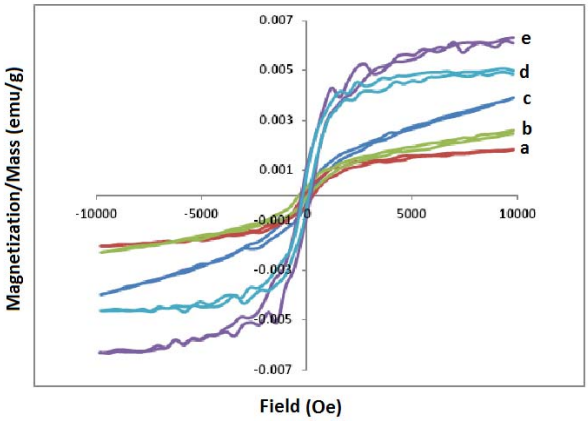

Fig.5. Room temperature field-dependent magnetization (M–H) for $Zn_{0.97}Co_{0.03}O$ thin films with different thicknesses (a) $300 \pm 20nm$ (b) $320 \pm 20nm$ (c) $480 \pm 20nm$ (c) $Zn_{0.94}Co_{0.06}O$ with $440 \pm 20nm$ thickness (d) $Zn_{0.91}Co_{0.09}O$with $455 \pm 20\,nm$ thickness

4. Conclusion

The $Zn_{0.97}Co_{0.03}O$ thin films were prepared on Si substrate using a PLD method with different thickness. The XRD patterns of the films showed ZnO hexagonal wurtzite structure and no cobalt oxide peaks were observed. It also showed that by increasing the thickness of the films, the (200) peak position is shifted a little to lower degrees, and the grain size parameter increased showing better crystallization of films with the increase of the thickness. From FESEM pictures and histogram particle size diagrams, it was estimated that the size of the particles on the surface rose in the range of 14 to 30 nm with increasing the thickness of the films. The optical measurement of the films indicated that the band gap of samples was reduced (~0.01 ev) by increasing the thickness. The films with 3% cobalt doped showed a superparamagnetic behavior. By increasing the concentration of cobalt in ZnO lattice, the thin films showed a weak ferromagnetic behavior with saturation magnetization about o.oo6 emu/g.

References

[1] M. Venkatesan, C. B. Fitzgerald, J. G. Lunney, J. M. D. Coey, Phys. Rev. Lett. **93**, 177206 (2004).
[2] K. Ando, H. Saito, Z-W. Jin, T. Kukumura, et al. Appl. Phys. Lett. **78**, 2700 (2001).
[3] P.V. Radovanovic, D.R. Gamelin, Phys. Rev. Lett. **91**, 157202 (2003).
[4] H. Saeki, H. Tabata, T. Kawai, Solid-State Commun. **120**, 439 (2001).

[5] K. Sato and H. Katayama-Yoshida, Jpn. J. Appl. Phys. **39**, L555 (2000).
[6] T. Shi, S. Zhu, Z. Sun, S. Wei, and W. Liu, Appl. Phys. Lett. **90**, 102108 (2007).
[7] F-Z. Ghomrani, S.Iftimie, N. Gabouze, A. Serier, M.Socol, A. Stanculescu, F. Sanchez, S.Antohe, M.Girtan , J Optoelectron. Adv. Mater. **5**, 257 (2011).
[8] S. Pilban Jahromi, N.M. Huang, A. Kamalianfar, H.N. Lim, M.R. Muhamad, R. Yousefi, Journal of Nanomaterials **2012**, 173825 (2012).
[9] K. Samanta, P. Bhattacharya, R. S. Katiyar, W. Iwamoto, P. G. Pagliuso,and C. Rettori, Phys. Rev. B **73**, 245213 (2006).
[10] J. H. Kim, H. Kim, D. Kim, Y. E. Ihm, W. K. Choo, Physica B. **327**, 304 (2002).
[11] A. Kamalianfar, S.A. Halim, S.P. Jahromi, M. Navasery, F.U. Din, K.P. Lim, S.K. Chen, J.A.M. Zahedi, Chinese. Phys. Lett. **29**(12), 128102 (2012).
[12] A. Khorsand Zak, M. Ebrahimizadeh Abrishami, W. H. Abd Majid, Ramin Yousefi, S. M. Hosseini,Cer. Inter. **37**, 393 (2011).
[13] J. Zhang, X.Z. Li, B. Xu, D.J. Sellmyer, Appl. Phys. Lett. **86**, 212504 (2005).
[14] H.J. Lee, S.Y. Jeong, C.R. Cho, C.H. Park, Appl. Phys. Lett. **81**, 4020 (2002).
[15] B.D. Cullity & S.R. Stock, Elements of X-Ray Diffraction, 3rd Ed., Prentice-Hall Inc. (2001).
[16] G.B. Williamson, R.C. Smallman, Philos. Mag. **1**, 34 (1956).
[17] T. Story, R. R. Galazka, R. B. Frankel, P. A. Wolff, Phys. Rev. Lett. **56**, 777 (1986).
[18] T. Dietl , J. Phys.: Condens. Matter. **19**, 165204 (2007).
[19] Q. Liu, C.L. Yuan, C.L. Gan, G. Han, J. Appl. Phys. **110**, 033907 (2011).
[20] T. Dietl , T. Andrearczyk, A Lipi´nska, M Kiecana, M Tay and Wu, Phys. Rev. B **76**, 155312 (2007).

*Corresponding author: ahalim@science.upm.edu.my